
Aluminum Zinc Oxide Transparent Conductors for Optical Cavity Enhanced Polymer Photovoltaics

Case Western Reserve
University Department of
Physics

Emily Griffin, Dr. Ken Singer

May 3, 2013

Abstract

Organic photovoltaic devices are a promising, renewable source of energy. Though they are easier to fabricate than inorganic devices, their efficiency must be increased before they become viable. This project focuses on characterizing Aluminum-doped Zinc Oxide for use as a transparent conducting oxide in these devices. The complex index of refraction, bulk resistivity, and transparency of the film must be determined, and its effect as part of an optical cavity must also be modeled using transfer matrix calculations. The optimal thickness for AZO is determined to lie between 300 and 600 nm, as the electrical and optical properties must both be optimized.

Introduction

Photovoltaic devices, also called solar cells, are a relatively recent source of renewable energy. The purpose of a solar cell is to convert solar energy to electrical energy. This is achieved by means of a semiconductor installed between two electrodes. When the sunlight strikes the semiconductor, it excites charge carriers, in the form of electrons and holes, from the valence band of the semiconductor into the conduction band. These can then move freely and migrate to the electrodes, where they will contribute to a current.

The semiconductor layer is called the active layer, because this is where the actual charge carrier migration takes place. It is made up of a donor material and an acceptor material. The donor material has energy levels which have lower-energy electrons that are more readily ionized, while the acceptor material has holes, or electron vacancies, which allow it to bind

electrons. A diagram of the energy levels of inorganic and organic semiconductors is shown in Fig. A below.

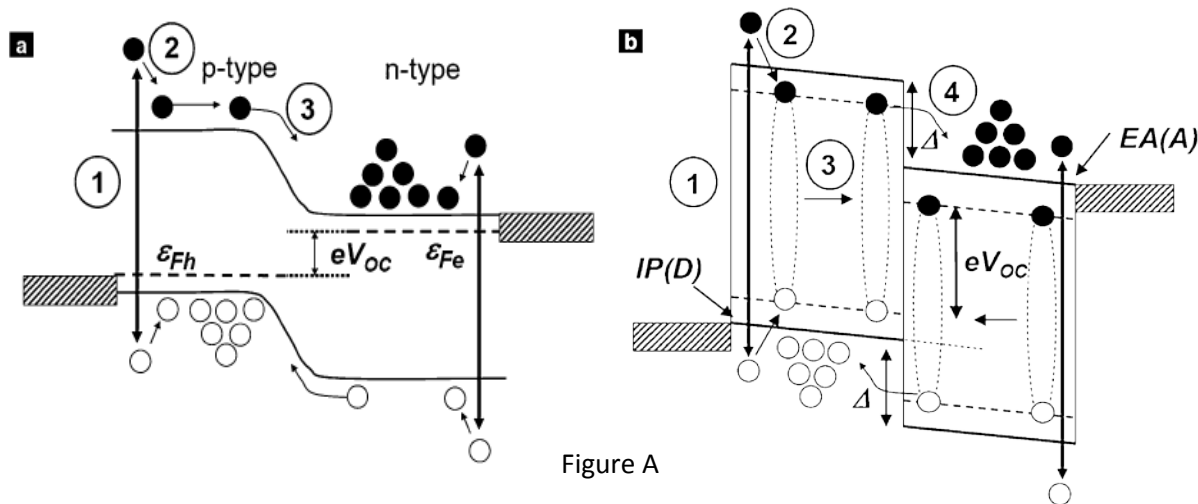


Figure A

a) inorganic energy level diagram: ϵ_{Fe} and ϵ_{Fh} are the quasi-Fermi levels which describe the population of electrons and holes. eV_{OC} is the open-circuit voltage. Steps 1-3 follow the energy transfer from the photon to the charge carriers in the semiconductor and the diffusion of minority charge carriers to the other material.

b) organic energy level diagram: $IP(D)$ stands for the Ionization Potential of the donor, while $EA(A)$ the Electron Affinity of the acceptor. eV_{OC} as before, where Δ is the difference between the donor and acceptor HOMO and LUMO, respectively. Steps 1-4 follow the energy transfer from the photon to the excitation and its diffusion to a boundary, where the minority carrier is again transferred to the other material.

Kippelen, Bernard and Jean-Luc Bredas. "Organic Photovoltaics." *Energy and Environmental Science* 2.3 (2009): 251-261. Print.

Traditionally, photovoltaics are made with inorganic semiconductors, generally silicon.

While these sorts of photovoltaics are well-developed and commercially available, there are disadvantages inherent in their design. The high temperature deposition process required for silicon leaves only a small range of substrates on which the devices can be fabricated. It also requires much more energy than a low temperature process, which is detrimental for a technology attempting to be a sustainable source of energy [1].

Organic photovoltaics can be deposited at low temperatures, allowing them to be manufactured on flexible plastic substrates, which can weigh less than the inorganic devices and are easier to install in a variety of settings, since they can be fit to surfaces which aren't flat. However, the power conversion efficiency of organic photovoltaics is not yet equal to that of the commercially available inorganic cells. Therefore, a variety of techniques are being utilized to increase this efficiency [1,2].

There are other difficulties inherent in organic photovoltaics – most notably, a length scale discrepancy between the diffusion length of the excitons (bound electron-hole pairs) excited by incident light and the thickness necessary in the active layer for good optical absorption. When the excitons form, they diffuse through the material and then recombine fairly quickly if they have not reached a p/n junction in the active layer. This recombination happens on the scale of 10-20 nm. However, the active layer must be on the order of 100s of nm in order to absorb a reasonable amount of light. This discrepancy can be solved by modifying the simple bilayers used for inorganic photovoltaics into a bulk heterojunction (BHJ) (see Fig. B). A heterojunction is a phase-separated mix of the donor and acceptor materials, allowing two length scales to coexist. The boundaries between the donor and acceptor materials can be accessed at the 10 nm scale, while the total heterojunction thickness is on the 100nm scale; hence its “bulk” characteristic. However, even with this arrangement, many excitations recombine and their energy is therefore not collected from the photovoltaic. Therefore, the thinner this BHJ can be, the better the cells' efficiency will be. Usually this means sacrificing absorption due to there being less material to absorb photons in a thinner active layer. However, if the absorption in

This, then, lets the BHJ reduce in thickness without sacrificing much in the way of absorption, while also gaining efficiency due to fewer excitation recombinations.

The optical cavity of this device has been modeled comprehensively by Brent Valle for the TCO Indium Tin Oxide (ITO). This modeling makes use of transfer matrix calculations, where the transmission, reflection, absorption, and electric fields are related using Maxwell's equations in the form of a matrix (or series of multiplied matrices). For each material in the device, the complex index of refraction is input to its own matrix, and together the matrices model the device. Modeling the device is useful in that the optimal thickness of different layers can be found without the necessity of fabricating many devices of varying thicknesses. Using this modeling method, Valle has calculated the optimal thickness of ITO to be anything between 50 and 140 nm, with an active layer (the organic semiconductor layer) thickness of around 80 nm [2,3].

Objectives

Though well-studied for ITO, this modeling process needs to be repeated for other TCOs. My project focused on Aluminum-doped Zinc Oxide (AZO) as a TCO, to be input into the transfer matrix model and then included in fabricated devices. AZO is cheaper than ITO partly because of the relative availability of indium compared to aluminum. ITO is also used in many other organic-based devices, such as organic light-emitting diodes and liquid crystal displays, which naturally limits the supply. AZO, on the other hand, is used much more frequently in photovoltaics than in any other device, so it is not as difficult or expensive to obtain.

The first objective was to sputter deposit the AZO on glass slides and measure its complex index of refraction. The thickness of the deposited films was investigated to determine which are electrically and optically reasonable for use in photovoltaics. To this end, the films should be both transparent and conductive. Spectroscopic ellipsometry was used to find the complex index of refraction of the films.

Next, this value was input into the transfer matrix model of the device and the spectra theoretically resulting from the device were calculated. Transfer matrices are essentially matrix handling of the calculation of fields based on Fresnel reflection and transmission coefficients. Since these depend on the index of refraction of the materials, this data is necessary for the calculation. More detail on transfer matrices is found below.

Finally, devices are designed based on the range of thicknesses for AZO and the active layer determined by the modeling calculations. The thickness of the AZO must meet requirements that it is both conductive and optically transparent, and the thickness of the active layer is chosen to be the most absorbing across a range of wavelengths.

Experimental

Fabricating Devices:

The device has the structure shown in Fig. C below, which is similar to that in Fig. B, but with the addition of an electron and a hole blocking layer. The active layer is made of poly-3-hexylthiophene, or P3HT, which is the donor material; and Phenyl C₆₀ butyric acid methyl ester, or PCBM, which is the acceptor material. The electron blocking layer is PEDOT:PSS and the hole

blocking layer is LiF, and are included to ensure that the charge carriers arrive at the correct electrodes. The cathode is Aluminum and the anode is Aluminum-doped Zinc Oxide, doped at 2 wt% Aluminum. The substrate must be transparent; it can be glass or, as previously mentioned, flexible plastic.

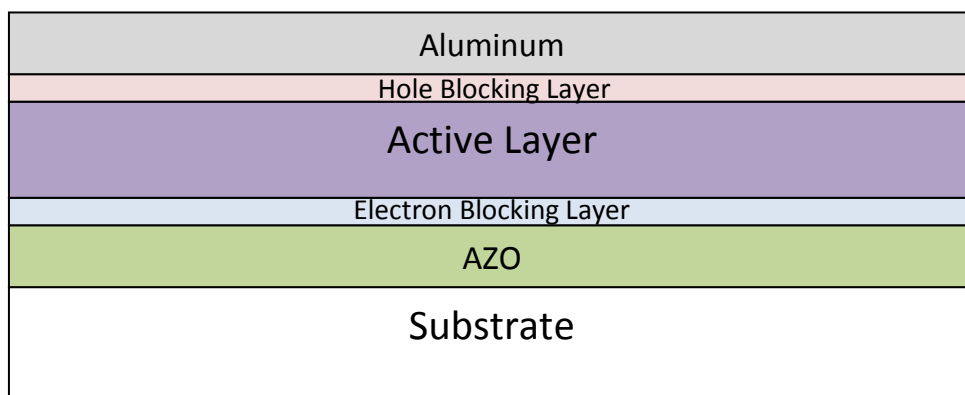


Figure C
Device structure

The glass substrate is first cleaned using repeated sonications: once in deionized (DI) water with 1% Liquinox detergent, twice in DI water, and once in acetone, methanol, and isopropanol, as well as an ultraviolet ozone cleaner. Then the TCO is sputtered onto the glass substrate, under deposition conditions described below. 40 nm of PEDOT:PSS is spin-cast and then annealed at 150° C for 10 minutes. The active layer, consisting of P3HT and PCBM, is also spin-cast and then allowed to dry for 30 to 60 minutes in an N₂ atmosphere. It is then annealed at 150° C for 5 to 10 minutes. A 1nm LiF layer and finally 120 nm of aluminum are thermally evaporated at about 1 x 10⁻⁶ Torr. The thicknesses of the layers are approximate, and those not specified depend on the calculations made during modeling [2].

Characterizing AZO:

The Aluminum-doped Zinc Oxide films were sputtered onto glass microscope slides using a DC sputtering system. They were deposited at room temperature and a base pressure of at least 2×10^{-6} Torr with nitrogen gas as the plasma source. The target was zinc oxide doped by 2 wt% Aluminum. The source-substrate distance was varied from 9 inches to 5 inches. Two samples were placed toward the edge of the substrate holder, and one in the center. All samples were measured with a stylus profilometer to find actual thickness, which was 320-385 nm for the larger source-substrate distance and 585-590 nm for the smaller distance. A spectroscopic ellipsometer was then used to measure the complex index of refraction of the film.

Ellipsometry measures a sample by shining a beam of linearly polarized light at the sample and analyzing its reflection to see how the polarization and intensity has changed. The raw data, in the form of two polarization angles ψ and Δ , is modeled to determine a best fit. This model is based on known information like the thickness and the type of model reasonable for the material. The AZO data is modeled using a parameterization of a standard Lorentz oscillator model for the interband absorption, with an added Drude oscillator component for the free carrier absorption [4].

The Lorentz oscillator takes the form of a Lorentzian curve, which fits the real part of the index of refraction from about 3 to 6 eV. The Drude oscillator is essentially a decay, which fits the imaginary part of the index of refraction from 1 to 3 eV, as can be seen in Fig. D. The bound state model is given by

$$n(\omega) = n_{\infty} + \frac{B(\omega + \omega_j) + C}{(\omega + \omega_j) + \Gamma_j^2}$$

$$k(\omega) = \begin{cases} \frac{f_j(\omega - \omega_g)^2}{(\omega - \omega_j) + \Gamma_j^2} & \omega > \omega_g \\ 0 & \omega < \omega_g \end{cases}$$

$$B = \frac{f_j}{\Gamma_j} [\Gamma_j^2 - (\omega_j - \omega_g)^2]$$

$$C = 2f_j\Gamma_j(\omega_j - \omega_g)$$

Where n and k are the real and imaginary parts of the complex index of refraction, n_{∞} is the long wavelength refractive index, ω_j the energy of maximum absorption, f_j the oscillator strength, ω_g the band gap energy, Γ_j the broadening factor, and ω the light energy. This is based on a parameterization by Fourouhi and Bloomer [4]. The free electron model fit (the Drude model) is given by

$$\frac{\omega_p^2}{-\omega^2 + i\Gamma_D\omega}$$

Where ω is still the light energy, ω_p is the plasma energy of the free electron gas, and Γ_D is the damping constant [4].

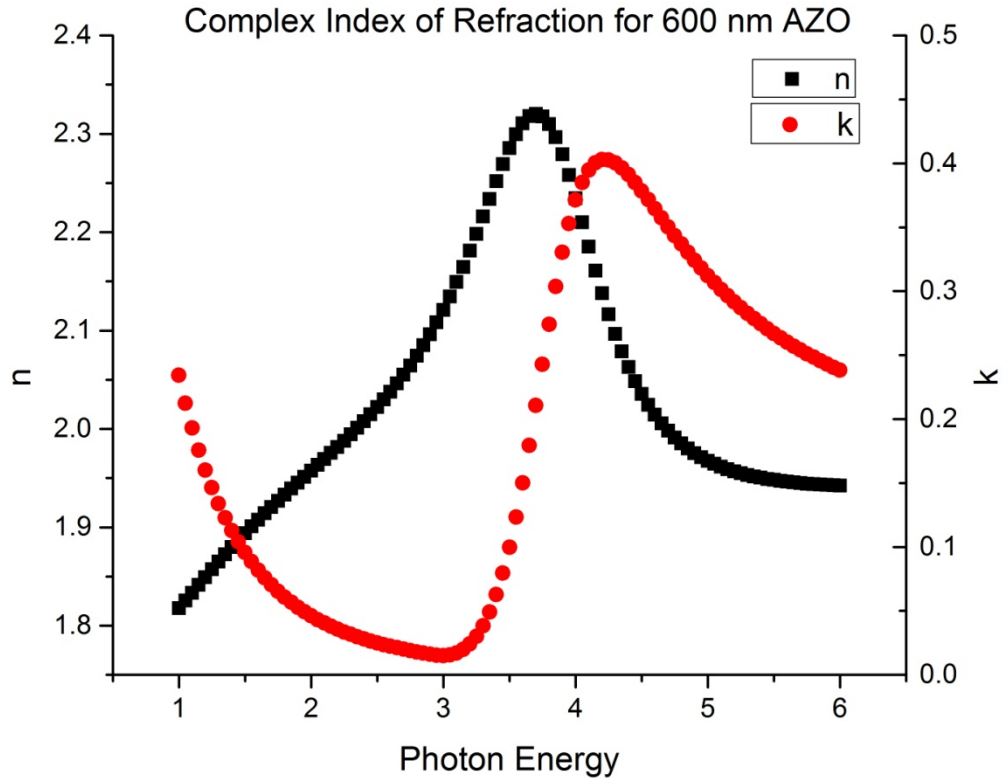


Figure D

Complex Index of Refraction for 600 nm AZO, plotted against photon energy. Note the Lorentzian form of the n centered around 3.7 eV and the Drude decay of the k from 1 to 3 eV.

There are also fit components to the model based on the properties of the other layers in the sample to be measured, including not only the relevant film layer but also the substrate and roughness of the film.

The values measured by the ellipsometer are two angles: ψ and Δ . They are related to the Fresnel reflection coefficients r_p (parallel component of reflection) and r_s (perpendicular component) by the following equation:

$$\rho = \frac{r_p}{r_s} = \tan\Psi \cdot e^{i\Delta}$$

Likewise, the real and imaginary part of the complex index of refraction, n and k , are related to these angles. It is this relation which we use to find their values from the raw data, once it has been fit well enough for data to be interpolated.

$$n^2 = \sin^2 \theta \left[1 + \tan^2 \theta \frac{(1 - \rho)^2}{(1 + \rho)^2} \right]$$

Where θ is the angle of incidence and ρ is as above.

Modeling Devices:

This complex index of refraction data is then input into the MATLAB code written to model the devices via a transfer matrix. The resultant matrix for a layered sample, as in this device layout, is determined by the number of interfaces and layers: each interface and layer has its own matrix to model the fields. Therefore, the fields can be written as the following matrix product:

$$\begin{bmatrix} E_0 \\ rE_0 \end{bmatrix} = \begin{bmatrix} M_{11} & M_{12} \\ M_{21} & M_{22} \end{bmatrix} \begin{bmatrix} tE_0 \\ 0 \end{bmatrix}$$

Where

$$M_{nm} = I_{nm} L I_{m,m+1}; \quad I_{nm} = \frac{1}{t_{nm}} \begin{bmatrix} 1 & r_{nm} \\ r_{nm} & 1 \end{bmatrix}; \quad L = \begin{bmatrix} e^{-ikL} & 0 \\ 0 & e^{ikL} \end{bmatrix}$$

$$t = \frac{1}{M_{11}}; \quad r = \frac{M_{21}}{M_{11}}$$

The M matrix is the product of matrices describing the field at each interface and in each layer.

The I matrix describes transmission and reflection at an interface and the L matrix describes

propagation through a layer of length L . This representation of the fields can be used to describe the field in the device as a whole, or in each layer individually.

This matrix can be used to calculate the absorptance (ratio of absorbed vs incident radiation) of a single layer. Absorptance in the active layer is most important, since this is where absorption of photons actually leads to a current. Therefore, we generate a graph of incident wavelength versus thickness of the active layer, with absorptance (ratio of absorbed vs incident radiation) plotted as a color gradient (see Fig. E for an example). This graph lets us design devices with the active layer thickness optimized for maximum absorptance across a range of wavelengths. The TCO thickness can also be varied plot by plot to compare which thickness yields the highest absorptance.

Results

Characterizing AZO:

The bulk resistivity and optical transparency for the two AZO film thicknesses were determined by a 4-point resistivity probe and a UV-Vis Spectrophotometer. The resistivity measurements for the ~ 300 nm sample ranged from 6700 to 20,000 Ω/square as deposited. After four 5-minute anneals at 300°C , one of the edge samples had a resistivity reduced to 170 Ω/square . The other edge sample was annealed 3 times at 350°C for 5 minutes and reached a resistivity of 77 Ω/square . The center sample was not annealed. After 4 days, the resistivity had increased to 1772 Ω/square for the first sample and 830 Ω/square for the second. The resistivity of the ~ 600 nm sample ranged from 33 to 53 Ω/square as deposited. Since the resistivity was already so low, these samples were not annealed. The first edge sample had a

resistivity of 39 Ω /square after deposition and 41 Ω /square after 9 days. The second edge sample had values of 42 Ω /square after deposition and 49 Ω /square after 9 days. The center sample measured 35 Ω /square after deposition and 46 Ω /square after 9 days.

Clearly, the ~600 nm sample was much more conductive than the ~300 nm sample. It also degraded much more slowly than the thinner sample, which means that it could still be used in devices several weeks after deposition. This thickness was better suited to function as an electrode.

The transparency of the different thicknesses was also measured. As the transparency varies over the entire spectrum of wavelengths from visible to UV light, the range over this wavelength span is quoted. For the thinner sample, transparency varied between 80% and 100% transparent. For the thicker sample, the range was 80% - 90%. Both samples are reasonably transparent, but the closer to 100% transparent the film is, the more light will be left to be absorbed in the active layer. Therefore, the thinner film is optically better suited to the device's construction.

The n and k data determined from the modeling of the spectroscopic ellipsometry data is given in Fig. D above. The real part, n , agrees well with literature in terms of its shape and range, while the imaginary part, k , agrees with the shape given in literature, but its values are slightly higher than those of the literature [5,6]. This means that the absorption in this material is slightly higher than the literature reports.

Modeling Devices:

Devices were modeled as consisting of a variable thickness of AZO, 40 nm of PEDOT:PSS, 0 – 400 nm of P3HT/PCBM and 120 nm of Al. The AZO thickness was varied from 100 to 800 nm in 50 nm intervals. The peak absorbance of the devices increased as the thickness decreased. However, the thickness of the active layer at which the peak thickness occurred varied with the thickness such that 150 nm AZO showed the thinnest high-absorbing active layer. As can be seen in Fig. E below, the absorbance shows periodic behavior at most thicknesses, with more pronounced periodicity at only several. This is the result of the optical cavity discussed above. Fig. E demonstrates the tuning of this cavity by comparing a device modeled with 100 nm AZO and 150 nm AZO; in the absence of an optical cavity, the graphs should look very similar, with possibly a uniform decrease in absorption as the thickness increased. But the graphs show different periodic behavior, with high levels of absorption at low thicknesses occurring over a much broader range of wavelengths in the device with the thicker AZO layer, not the thinner one. This occurs because the device with this thickness is tuned to a resonant frequency of the cavity, and so the absorption in the device is higher.

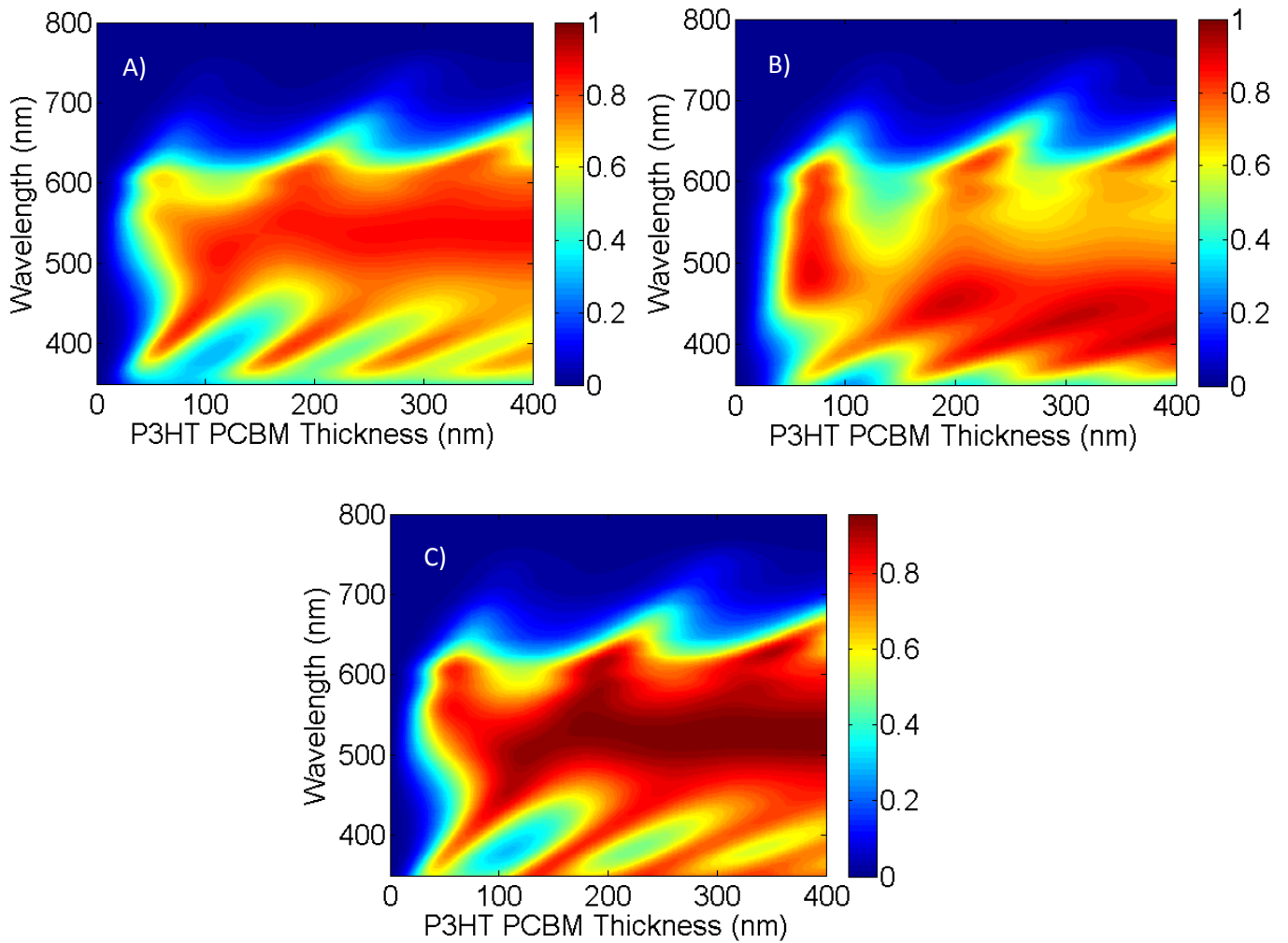


Figure E

Plots of the absorbance (color bar) of the active layer as a function of incident wavelength and active layer thickness. A) is for a device with thickness 150 nm AZO and B) for 100 nm AZO with all other parameters held constant. Note the absorbance pattern at low wavelengths and around 50 nm P3HT PCBM thickness. Plot C) compares the plot of 150 nm ITO with all other parameters the same. This is clearly more absorbing than the AZO device A) at the same thickness.

Optically, then, we can determine that the AZO layer thickness should be around 150 nm so as to take advantage of the wide absorbance spectrum demonstrated at even very thin active layer thicknesses. Comparing this to the optimal thickness of the previously used oxide, ITO, shown in Fig. E above, we can see that the absorbance is not as high as for that device, even at the same thickness. This is most likely because the AZO traps more of the light than the ITO does, leaving less light to be absorbed in the active layer.

Conclusions

Based on the optical characterization of the AZO and the device modeling described above, we find that, optically, the optimal thickness for a TCO made from AZO is 150 nm. However, the resistivity of the material at that thickness is not low enough to allow for good conduction of the charge carriers released by the photons. Based on the electrical characterization of the AZO, we find a thickness around 600 nm to be electrically optimal for a TCO made from AZO. Therefore, the thickness of the AZO actually used in fabricating the devices should be somewhere between these two values, and should balance the requirements of the optical and electrical properties. As the number of data points on the resistivity is small, the estimate can only be narrowed to be between 300 and 600 nm.

With this estimate, this project has contributed to the increased efficiency of organic photovoltaic devices by investigating a new transparent conducting oxide for use in these devices and determining its properties: individually and as part of the device structure. In comparison, AZO seems to render the device less absorptive for the same range of thicknesses, and would need to be fabricated with a thicker oxide layer, which would leave it even less absorptive. An analysis of the cost benefits of AZO would have to be done before concluding whether AZO is a better option than ITO. The optical cavity effect is seen with this material as well as with ITO, which reinforces the relevance of its consideration in OPV architecture.

Future Work

The next step is to fabricate devices. Several intermediate steps must first be taken, however: as the conclusion suggests, the conductivity of a wider range of film thicknesses

should be probed, in order to determine the thinnest film which will still demonstrate a bulk resistivity in the 10s of Ω/square . This film should be modeled with the transfer matrices and the appropriate thickness of the active layer must be determined.

Before actually fabricating devices, a small study must be carried out as to how the various polymers spin-cast onto AZO, as the current data is only for ITO and the recipe reflects this. Once thicknesses can reliably be fabricated, the device should then be made and tested. The device's I-V curve and External Quantum Efficiency (ratio of incident photons to resulting charge carriers) should be measured and compared to current devices. Hopefully, the devices fabricated with AZO will exhibit similarly efficient results to those utilizing ITO, though the transfer matrix calculations suggest otherwise.

Acknowledgements

I would like to thank my advisor, Dr. Kenneth Singer, and his graduate students Brent Valle and Rosemary Bramante, as well as the director of the Materials for Opto/Electronics Research and Education Center, Ina Martin.

References

- [1] Kippelen, Bernard and Jean-Luc Bredas (2009). Organic Photovoltaics. *Energy and Environmental Science*, 2(3), 241-332.
- [2] Brent Valle, et al. (2012). Spectral aspects of cavity tuned absorption in organic photovoltaic films. *Optics Express*, 20(S6), A954-A963.
- [3] Yeh, Pochi (1998). *Optical Waves in Layered Media*. Hoboken: John Wiley & Sons, Inc.
- [4] Horiba Jobin Yvon Spectroscopic Ellipsometry User Guide (2008).
- [5] Gao, Xiao-Yong, Yan Ling, and Qing-Geng Lin (2010). Analysis of the optical constants of Aluminum-doped Zinc-oxide films by using the Single-oscillator Model. *Journal of the Korean Physical Society*, 57(4), 710-714.
- [6] A.C. Galca, et al. (2010). Optical properties of zinc oxide thin films doped with aluminum and lithium. *Thin Solid Films*, 518, 4603-4606.